Inverse control applied to structural excitation systems

Marco Norambuena, René Winter, Jörn Biedermann
Institute of Aeroelasticity, German Aerospace Center (DLR), 37073 Göttingen
E-Mail:Marco.Norambuena@dlr.de

Abstract

Accurate control over excitation sources is a necessary requirement for the study of structure-borne noise mechanisms. This is especially true when the main focus is set on the influence of real operational forces acting on the structure. Under laboratory tests, it is not always possible to have real operational conditions. A relevant case is an aircraft engine attached to a wing, where it is necessary to reproduce the operational forces on the structure without having an engine available. The defined task is to accurately reproduce excitation forces that were previously obtained from simulations. For this purpose, it is possible to use an adaptive controller to drive a shaker that will inject into the structure an exact copy of the reference forces already calculated. The main objective of the controller is to compensate the transfer function created between exciter and structure in order to generate the previously simulated loads at the attachment points. The following work presents the development of such adaptive controller and the laboratory tests performed in order to validate the proper operation of the system. As a first step in the development of the control system, a SISO controller is used in combination with a generic structure.

Introduction

In the aeronautics industry, Ground Vibration Tests (GVT's) are a well stablished testing procedure meant to characterize structural behavior of aircrafts. Such applied methodology serves as key part not only in the understanding of aeroelastic stability but also provides relevant data used to validate analytical models that ultimately become part of the certification process of airworthiness [1]. In summary, GVT's are able to accurately describe the fuselage response by means of artificial excitation of the structure. There are two other closely related methods to achieve similar objectives, Taxi Vibrations Tests (TVT) and Flight Vibrations Tests (FVT), the former consists in the replacement of the artificial shaker excitation by the natural vibrations generated during aircraft taxiing [2] and the later uses the operational vibration generated on the fuselage during flight [3].

Any current structural testing procedure in the field of aeronautics uses one, or a variation, of these methods. From the excitation point of view, the most common strategy is to use arbitrary, but known, excitation signals, e.g. white noise or sine sweeps. This provides the necessary flexibility to obtain, for instance, frequency response functions, modal parameters, etc.

One could easily argue that a FVT will provide the perfect type of excitation since it is in fact an operational condition, however the elevated costs associated with flight tests make this option unfeasible in most cases. Moreover, such type of excitation, although ideal for many applications, is completely unknown and difficult to quantify since there are multiple sources acting on the fuselage during flight. The unavailability of such excitation reference will limit the types of processing that can be performed, e.g. modal masses can't be obtained.

During recent years [4], vibroacoustic topics had drawn considerable attention in the aeronautic industry. This is given by the fact that concerns have been shifted from safety and reliability topics of previous decades of research to cabin quality and passenger comfort. This current trend has pushed the development of new tools and methodologies in order to face these new challenges [5]. A set of refocused topics has emerged from the interest in understanding how vibroacoustics play a crucial role in the cabin noise.

Given the fact that the starting points of all vibroacoustic phenomena are vibrations propagating on a structure, it is necessary to have a suitable excitation system capable of reproduce real flight operational conditions. If we forget for one second the effect of the Turbulent Boundary Layer, the solely source responsible for vibrations on the fuselage at low frequencies are the loads generated by the rotating components of the engines.

Through simulation, it is possible to accurately calculate the loads generated at connection points between engines and fuselage. However, a key problem arises at the moment when you try to reproduce those loads on the structure, since there is no way to compensate for the modifications introduced by the system created between amplifier, shaker and structure. Such unaccounted system will certainly change the predefined reference loads. Nonetheless, if the reference loads signal is available, it can be used to design an active excitation system able to generate and inject into the structure an exact copy of the simulated loads. As we will show in the following sections, such real-time excitation system is based on an adaptive controller. Although our long-term goal is the implementation of a multichannel system able to reproduce forces in the three directions of space plus its associated moments, creating a multi-input multi-output system, the first step in this direction is the realization of a single channel controller (SISO) that serves as a proof of concept and will be the core for the future work.

Therefore, if we could implement a system able to excite a structure in a realistic manner, mimicking true loads, such system will allow to study the vibroacoustic behavior of a structure in the most accurate way possible. Such opportunity will help, for example, in the better understanding of structure—borne noise mechanisms of different parts of a fuselage or will assist in the determination of relevant energy transmission paths between sources and receivers.

Controlled excitation

The type of problem presented in this scenario, where it is required to inject on a structure a copy of an arbitrary reference force signal, seems to be a perfect candidate for an active control solution. The two main reasons for this are the availability of a reference signal, in this case the load forces, and the need to compensate a relatively stable plant. In this particular case the plant consists of the path created between amplifier, electrodynamic shaker, the structure and a force cell used to quantify the injected force, Figure 1 shows the configuration of the plant.

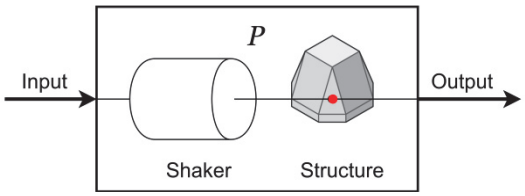

Figure 1: Schematic of the plant which consists of a shaker, a structure and a force cell (denoted by the red dot) that quantify the injected force into the structure.

The type of configuration described above is known as inverse control, since the task of adaptive process is to generate an inverse system $\hat{C}$ of the plant P. If this is successfully accomplished, the output of the plant will be an unmodified copy of the reference force signal. The typical schematic of an idealized inverse controller is shown in Figure 2, where $\hat{C}$ represents the compensation filter of the plant P, driven by the adaptive procedure. The error signal represents the deviation of the output of the plant in comparison with the reference force signal at the input of $\hat{C}$.

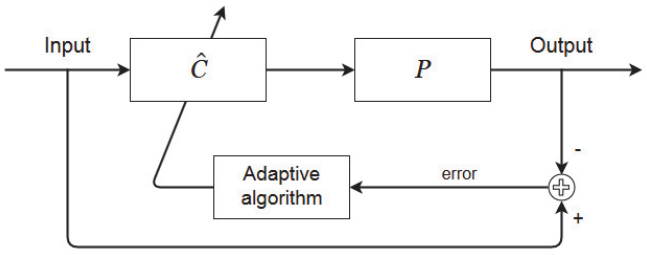

Figure 2: Diagram of an idealized adaptive inverse controller.

There are multiple options available to implement the adaptive algorithm. From the most simple and reliable LMS variations to the most sophisticated and demanding RLS variations.

According with this type of application, the following algorithms were tested in order to find the best tradeoff between speed of convergence and overall quality of output signal: NLMS, Correlation-LMS, DCT-LMS and RLS. The comparisons showed that all algorithms performed fairly well. After this comparison and considering that there is no requirement of high speed tracking of the reference signal, it was decided that the NLMS was the proper choice at this stage. Having the simplicity of an NLMS algorithm will make it easier to debug any problem that could potentially appear during the implementation on hardware.

The idealized system shown in Figure 2 is the most basic configuration for an inverse controller. However this simplicity helps to illustrate how such configuration works. Unfortunately, such idealized controller is not able to work properly on a real implementation since it requires conditions that are almost impossible to obtain, e.g. that there is no internal disturbance at the output of P. One of the options suggested in the literature [6] that can be used for an actual implementation, has a configuration similar to what is called *filtered-x* LMS (Fx-LMS) algorithm. This configuration is well known and widely used in Active Noise Control applications [7].

One of the characteristics of this configuration is that the control filter $\hat{C}$ is not applied directly to the plant P but rather to a modeled version $\hat{P}$ of the plant. The Fx-NLMS configuration ensures stable inverse control of the plant even in the case where there are errors in the modeling of $\hat{P}$. Independently of how $\hat{P}$ is modeled, online or offline, the complete control system can be summarized in Figure 3. In this schema it is assumed that on a previous process the plant $\hat{P}$ was identified and now a copy is connected at the input of the control filter $\hat{C}$. Under certain conditions it could be desired that the plant does not track directly the *Reference* signal but rather a delayed or modified version of the *Reference*. The introduction of the *Reference model M* serves this purpose.

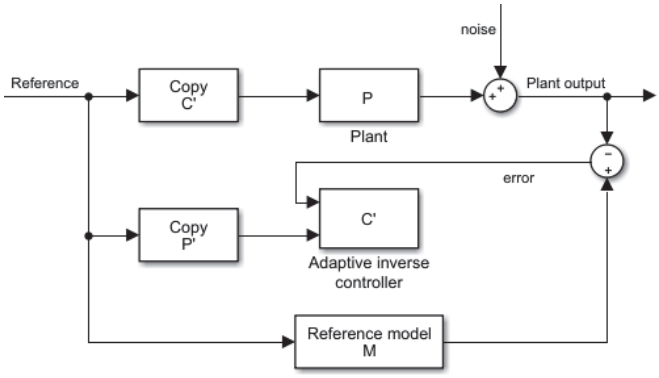

Figure 3: Diagram of inverse controller with added reference model.

Simulations

Although multiple simulations were performed during the development processes in order to test different algorithms, a simple example is presented here for the purpose of illustrating the general behavior of the controller. In this example, an arbitrary plant P with a low-pass characteristic was chosen. This fact is evidenced by the spectral profile of the *Control OFF* curve in Figure 5, which will be discussed shortly. The reference signal was defined as the sum of four sinusoids with frequencies 30, 50, 170 and 240 Hz.

In the following figures, time and frequency comparisons are presented between the *Reference* that represents the desired signal that should be injected into the structure, *Control OFF* that represents the signal obtained at the output of the plant when no control is performed (bypassing $\hat{C}$) and *Control ON* is the same as the latter but now the controller $\hat{C}$ is operating. All these curves are shown in Figure 4 and Figure 5. The

time domain comparison, in Figure 4, presents two important characteristics, firstly, the evident difference between the *Reference* signal and the *Control OFF* signal given by the effect of the transfer function of the plant *P*. This means that when there is no control applied, the injected signal into the structure does not resemble the predefined *Reference* signal. The second characteristic worth to mention is the evolution of the *Control ON* signal and its convergence to the *Reference* signal as time passes. This means that, as it was designed, after some time the controller $\hat{C}$ will compensate the influence of the plant *P* and will inject a proper copy of the *Reference* signal into the structure. The spectral comparison presented in Figure 5 shows a similar result, a disparity between *Reference* and *Control OFF* signals; and subsequently a perfect matching between *Reference* and *Control ON* signals.

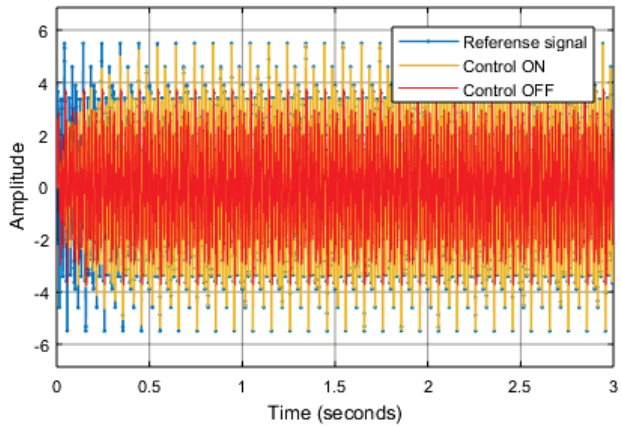

Figure 4: Comparison of signals evolution.

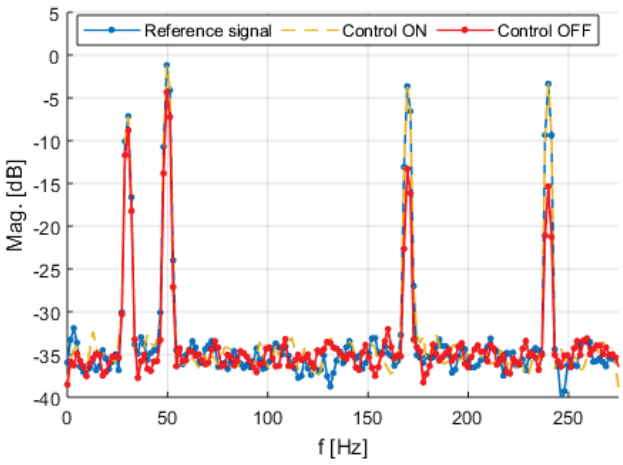

Figure 5: Comparison of resulting spectra.

The task performed by the adaptive filter $\hat{C}$ can be described by the evolution of its coefficients. Equally important, at the core of the adaptive process is the evolution of the error signal, which is responsible for driving the coefficients of $\hat{C}$ in the update equation of the LMS algorithm. The relationship between the progression of the error and the controller $\hat{C}$ can be observed in Figure 6.

Hardware realization and Experimental results

The last stage in the development process of the active controller was the implementation of the previously described algorithm into specialized hardware running in real time. The whole controller was implemented in two separate steps, firstly the plant *P* was identified and then a copy of *P* was used to run the Fx-NLMS inverse control. For this purpose the algorithm was developed using Simulink and an ADwin-Pro II system.

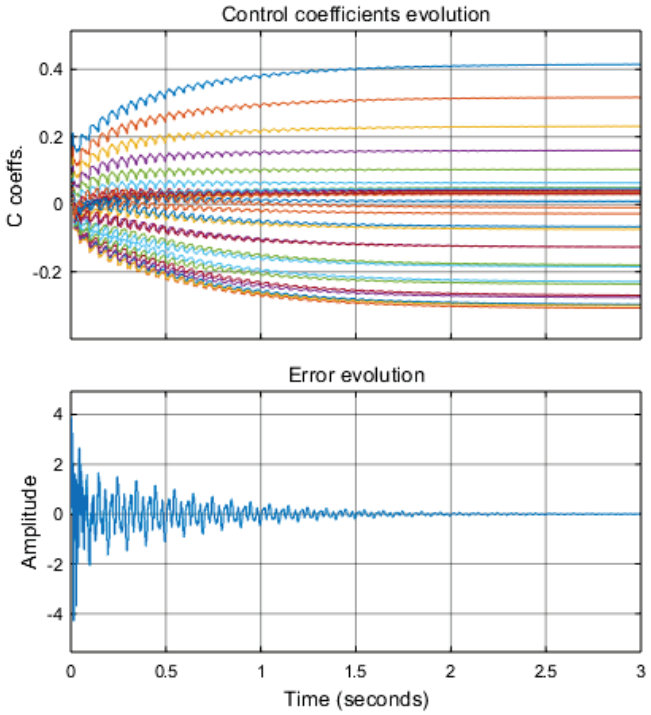

Figure 6: Illustration of error and coefficients evolution of the presented simulation.

In order to evaluate the correct operation of the system, a laboratory experiment was designed. The idea was to define a reference signal with a narrow band profile that resembles a low pass filter characteristic but with a non-flat response, as seen in Figure 7. In this way, the performance of the controller will be evaluated under, although limited, broadband condition that is still relevant for the use cases of structural excitation. The chosen frequency range was from 0 to 120 Hz.

The test structure used was a single aluminum plate of 1 x 0.8 x 0.03 m, with an asymmetric milled pattern that resembles the skin fields, stringers and frames typically found in fuselage structures. The thickness of the skin fields, stringers and frames was 1, 5 and 10 mm respectively. The plate was suspended using bungee cords in order to generate free displacement boundary conditions. As seen in Figure 8, a shaker and an impedance head were screwed to an anchor point of the plate. From the impedance head, the force signal was used to generate the error signal by comparing the actual injected force with the predefined force reference signal.

A spectral comparison of the reference and control signals is shown in Figure 7; there it is possible to assess the correct operation of the controller under narrow band excitation. In addition, a second evaluation is made by calculating the transfer function between the input and the output of the whole system, from the *Reference* signal fed into the controller $\hat{C}$ up to the output of the plant using the signal coming from the force cell. As before, two conditions are evaluated, *Control ON* and *OFF*. The comparison of the frequency response function for both conditions is made in terms of their magnitude and phase, as shown in Figure 9. The results presented there provide evidence about the

correct operation of the controller. Firstly, the adjustment of the magnitude around 1 means a close match between the injected force into the structure and the predefined reference. Secondly, a similar behavior takes place with the phases of both cases, where the *Control ON* condition displays a relatively flat line around 0 rad. All this means that the controller is properly working and is able, for the most part, to calibrate the injected force using the predefined *Reference* signal.

There are, however, three distinctive peaks that appear in the higher frequency region, this peaks are associated with the natural modes of the plate. Their presence there is somewhat expected; it is possible to identify two important factors that can influence their appearance here. In the first place, the structure used is highly undamped which can greatly increase the interaction between the injected force and response of the plate. Near resonances, any small out-of-phase displacement between the structure and the force cell can generate a seemingly large signal at the output of the force cell. Secondly, the assumption that the shaker is behaving as a linear time invariant (LTI) system is not necessarily true, at least up to some degree. One option to minimize this effect could be to perform an online identification of the plant $\hat{P}$ in order to compensate any variation over time while the inverse controller is running.

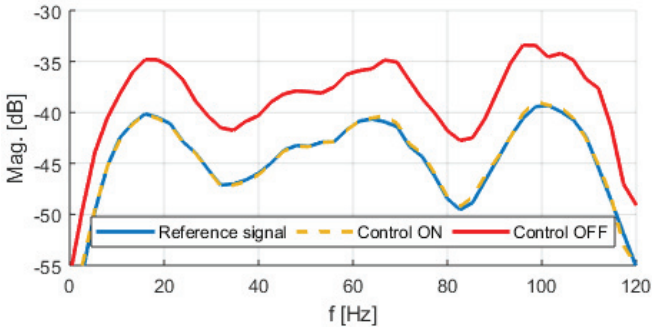

Figure 7: Spectral comparison of reference and control signals.

Figure 8: Aluminum plate used as test structure.

Concluding remarks

In this paper we examine the application of an active system to perform controlled structural excitation. Simulations and laboratory test show that it is possible to successfully apply a calibrated excitation for either multi-tonal or broadband signals in accordance with an arbitrary predefined reference. Future work will move forward by improving control around resonances and extending the current system to a multi-input multi-output controller.

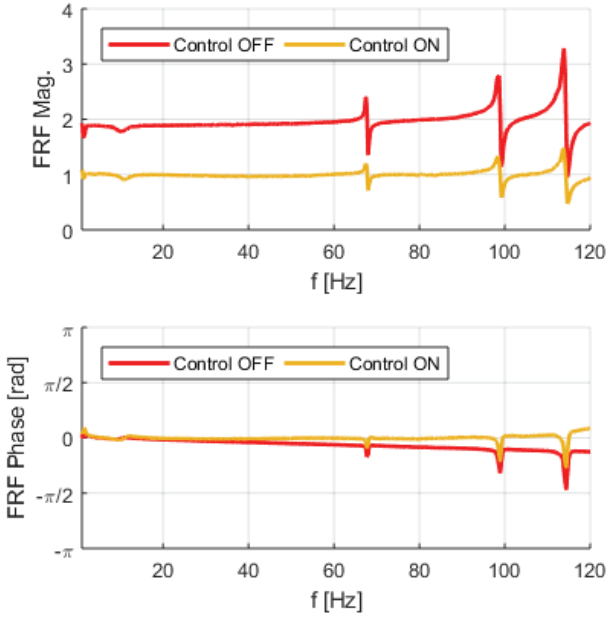

Figure 9: Frequency response function comparison in terms of magnitude and phase relatively to the reference signal.

Acknowledgement

This project has received funding from the Clean Sky 2 Joint Undertaking under the European Union's Horizon 2020 research and innovation programme under grant agreement No CS2-LPAGAM- 2014-2015-01.

Bibliography

[1] D. Göge, M. Böswald, U. Fullekrug and L. Pascal, "Ground Vibration Testing of Large Aircraft - State-of-the-Art and Future Perspectives," in *Proceedings of the 25th International Modal Analysis Conference (IMAC XXV)*, Orlando, 2007.

[2] M. Böswald and Y. Govers, "Taxi Vibration Testing - An Alternative Method to Ground Vibration Testing of Large Aircraft," in *Proceedings of the International Conference on Noise and Vibration Engineering - ISMA 2008*, Leuven, 2008.

[3] J. Meijer, "Introduction to Flight Test Engineering - "Aeroelasticity"," RTO AGARDograph 300 Vol. 14, 2005.

[4] J. Biedermann, R. Winter, M. Norambuena and M. Böswald, "Classification of the mid-frequency range based on spatial Fourier decomposition of operational deflection shapes," in *24th International Congress on Sound and Vibration (ICSV24)*, London, 2017.

[5] R. Winter, J. Biedermann, M. Böswald and M. Wandel, "Dynamic characterization of the A400M acoustics fuselage demonstrator," in *Inter-Noise 2016*, Hamburg, 2016.

[6] B. Widrow and E. Walach, Adaptive Inverse Control, Prentice-Hall Inc., 1995.

[7] S. Elliott, Signal Processing for Active Control, London: Academic Press, 2001.